Article

Journal of
Nanoscience and Nanotechnology
Vol. 18, 951–958, 2018
www.aspbs.com/jnn

Peroxidase-Like Activity of Gold Nanoparticles and Their Gold Staining Enhanced ELISA Application

Doudou Lou[1], Yanyan Tian[1], Yu Zhang[1,*], Junjie Yin[2], Ting Yang[1], Chuan He[1], Ming Ma[1], Wei Yu[3], and Ning Gu[1,*]

[1] *State Key Laboratory of Bioelectronics, Jiangsu Key Laboratory for Biomaterials and Devices, School of Biological Science and Medical Engineering, Southeast University, Nanjing 210096, P. R. China*
[2] *Center for Food Safety and Applied Nutrition, Food and Drug Administration, College Park, Maryland 20740, United States*
[3] *Research Institute of Clinical Laboratory Medicine, Jinling Hospital of Nanjing, Medical School of Nanjing University, Nanjing 210002, P. R. China*

We found that the peroxidase-like activity of gold nanoparticles (GNPs) followed the Michaelis-Menten kinetic model and was dependent on environmental pH and temperature, which was very similar to natural Horseradish Peroxidase (HRP). However, unlike HRP, which needs a lower H_2O_2 concentration with a very narrow range to reach a maximum reaction rate and avoid enzyme poisoning, GNPs have very high activity, even at an H_2O_2 concentration two orders of magnitude higher than HRP. It was demonstrated that H_2O_2 treatment could enhance the peroxidase-like activity of GNPs, resulting thus in the activity increase in a circular catalytic reaction by the reduplicative use of GNPs. It was also found that the peroxidase-like activity of GNPs responded sensitively to nanoparticle size and surface modifications. When used in an immunoassay, GNPs were generally conjugated with antibody and blocked with hydrophilic macromolecules to construct a nanoprobe. This strongly reduced the peroxidase-like activity and detection sensitivity of GNPs, therefore, restricting their use as peroxidase mimetics. We presented a novel strategy that combined the nanoprobes with gold staining to expose fresh catalytic gold surfaces and obtained a great increase in detection sensitivity.

Keywords: Gold Nanoparticles, Peroxidase-Like Activity, Gold Staining, ELISA.

1. INTRODUCTION

Natural enzymes, which possess high substrate affinity and efficiency in catalytic reactions under mild conditions, have been widely studied as catalysts. However, natural enzymes are difficult to extract and easy to deactivate in unfavourable conditions,[1,2] artificial enzymes need to be developed to duplicate the advantages of natural enzymes but avoid their disadvantages and are more affordable as well.

Nanostructures have attracted great attention because of their unique electrical, magnetic, optical, catalytic and other physical and chemical properties.[3–5] The intrinsic peroxidase-like activity of magnetite nanoparticles (MNPs) was discovered by the Yan Group,[6] which exhibits a great potential for special immunoassays when conjugating MNPs with antibody, with simultaneous capture, separation and detection capabilities. This finding provided a new idea that the nanoparticles could be used as new detection tools in biological diagnosis. Afterwards, there were more studies on nanostructured enzyme mimics as diverse as V_2O_5 Nanowires,[7] Prussian blue nanoparticles,[8] Hemin-Graphene Hybrid Nanosheets,[9] apoferritin-platinum nanoparticle composites (Pt–Ft)[10] and Au@Pt nanorods.[11,12] Gold nanoparticles, as a kind of famous functional nanomaterials, have been widely applied in biological and chemical detection due to their unique surface plasmon resonance (SPR) and surface chemical properties. They are generally modified with biocompatible molecules, such as glucose oxidase, immunoglobulin G (IgG), protein A, and human chorionic gonadotrophin to construct specific gold nanoprobes.[13–15] These gold nanoprobes can be easily detected by spectrophotometry, transmission electron microscopy (TEM), inductively coupled plasma-mass spectrometry (ICP-MS), electrochemical analysis, and light scattering analysis.[16] Therefore, they are important tools for developing

*Authors to whom correspondence should be addressed.

immunoassay and DNA hybridization detection methods. Because of their size and surface effects, gold nanoparticles can also be used in catalysis, especially for environmental and biological applications. Recently, GNPs were found to have intrinsic catalytic activity for H_2O_2 decomposition and superoxide scavenging at different pHs by using electron spin resonance spectroscopy (ESR),[17] meaning that GNPs might be used for new detection methods based on their enzyme-like activity. But the sensitivity of immunoassays catalyzed by nanoparticles as peroxidase mimetics or labels is limited due to their surface modifications with biomacromolecules which prevent the surface catalytic reaction.[6] In other words, the active centers of nanoparticles were blocked by antibodies and other protein modifications on their surfaces.

In this study, we considered gold nanoparticles as pH-dependent enzymes that could mimic peroxidases in an acid environment. Then we discovered that they could be reused as peroxidase mimetics and had peroxidase-like activity in biodetection, that is, they could be used in ELISA assays instead of HRPs. Gold staining, a procedure for electroless deposition of reduced gold irons where the GNPs act as nuclei, was established to reverse the negative effects of antibody surface modifications and increase the positivity/negativity (P/N) ratio. In this technique, the antibody conjugated gold nanoprobes act as detection labels and catalyst nuclei. They adsorb gold ions and promote their reduction into the surface of metallic gold nuclei. The process increases the amount of freshly exposed gold surface and accelerates catalysis of chromogenic substrates during biodetection.

2. MATERIALS AND METHODS

2.1. Materials

Working solutions of H_2O_2 were prepared fresh from 30% (v/v) H_2O_2 (Aladdin Co. Ltd., China). 3,3′,5,5′-teramethylbenzidine (TMB) and 2,2′-azino-bis (3-ethylbenzthiazoline-6-sulfonic acid) diammonium salt (ABTS) were both purchased from Alfa Aesar. Gold chloride tetrahydrate ($HAuCl_4 \cdot 4H_2O$) was obtained from Shanghai Reagent (Shanghai, China). Hexadecyltrimethyl ammonium bromide (CTAB) was obtained from Aladdin Co. Ltd., China. Trisodium Citrate ($Na_3C_6O_7$), hydroxylamine hydrochloride ($NH_2OH \cdot HCl$), dimethyl sulfoxide (DMSO), anhydrous sodium acetate (NaAc) and acetic acid (HAc) were purchased from Guoyao Co. Ltd., China. Anhydrous potassium carbonate (K_2CO_3), potassium chloride (KCl), sodium chloride (NaCl), sodium phosphate dibasic (Na_2HPO_4) and monopotassium phosphate (KH_2PO_4) were reagents from Shanghai Lingfeng Chemical Reagent Co. Ltd., China. Goat anti-human IgG was purchased from Bethyl Laboratories (Montgomery, TX, USA). Human IgG, bovine serum albumin (BSA), and Tween-20 were obtained from Kaiji Biotechnology Co. Ltd., China. All the reagents were of analytical grade and ultrapure water obtained from a Millipore Milli-Q water purification system was used throughout the experiments. Polystyrene 96-well microtiter plates (Costar) were used to perform the immunoreactions.

2.2. Synthesis and Characterization of GNPs

2.2.1. Synthesis of GNPs of Different Sizes

The colloidal solutions of 14, 25, 48, and 99 nm diameter GNPs were synthesized by the citrate reduction method as previously described.[18] Briefly, 1 mL of 1% $HAuCl_4$ solution was added into 97 mL of ultrapure water and heated to boiling, then 2 mL of 1% trisodium Citrate solution was added to the reaction system quickly, keeping boiling for 15 min. The different sizes of GNPs were obtained by adjusting the proportion of sodium citrate and $HAuCl_4$ in the reaction system as shown in Table I. The Au concentrations were all unified 47.8 $\mu g \cdot mL^{-1}$.

2.2.2. Characterization

UV-vis absorption spectra were obtained with a Shimadzu UV-3600 spectrophotometer. Transmission electron microscopy (TEM) analysis was performed on a JEM-2000EX microscope.

2.3. Kinetic Analysis

Unless otherwise stated, steady-state kinetic assays were carried out at 25 °C in a 96-well plate, with 50 μL of GNPs (14 nm, 47.8 $\mu g \cdot mL^{-1}$) in 200 μL of reaction buffer (0.2 M HAc-NaAc, pH = 3.6) in the presence of H_2O_2, TMB and ABTS. The kinetic analysis of GNPs with TMB as the substrate was monitored by adding 12 μL of 30% H_2O_2 and different amounts (0, 0.2, 0.4, 0.8, 1.6, 2.4, 3.2, 4, 5 μL) of TMB solution (10 $mg \cdot mL^{-1}$, dissolved in DMSO). The kinetic analysis of GNPs with H_2O_2 as the substrate was monitored by adding 3.2 μL of TMB and different amounts (0, 0.7, 1.5, 3, 6, 12, 18, 24, 32 μL) of 30% H_2O_2 solution. The reactions were monitored at 650 nm by the microplate reader (BIO-RAD model 680) after the substrates were added. The kinetic analysis of GNPs with ABTS as the substrate was performed by adding 32 μL of 30% H_2O_2 and varying amounts (0, 0.5, 1, 2, 4, 6, 8, 10 μL) of ABTS solution (10 $mg \cdot mL^{-1}$, dissolved in ultrapure water). The kinetic analysis of GNPs with H_2O_2 as the substrate was performed by adding 10 μL of ABTS and varying amounts (0, 2, 4, 6, 8, 12, 32, 64 μL) of 30% H_2O_2 solution. The reactions

Table I. Relationship between the size of GNPs and the ratio of reactants.

Volume of 1% $HAuCl_4$	Volume of 1% trisodium citrate	Size of GNPs
1	5	14
1	1.5	25
1	1	48
1	0.42	99

were monitored at 410 nm by the microplate reader after the substrates were added.

The apparent kinetic parameters were calculated based on the Michaelis-Menten Eq. (1),

$$V = \frac{V_{\max} \times [S]}{K_m + [S]} \quad (1)$$

where V is the initial velocity, $V_{\max}$ is the maximal reaction velocity, $[S]$ is the concentration of substrate and K_m is the Michaelis constant.

2.4. The Reusability of GNPs in Catalytic Reaction

The reusability assays were carried out using 300 μL of GNP solution (14 nm, 47.8 $\mu g \cdot mL^{-1}$) in 1.2 mL of HAc-NaAc buffer (0.2 M, pH = 3.6), with 546 μM ABTS substrate at 25 °C. The H_2O_2 concentration was 1.87 M. The reactions were monitored using the UV-vis spectrophotometer for 20 min, and then GNPs were collected by centrifugation and used as catalysts again. The procedure above was repeated until the catalytic activity of GNPs decreased.

2.5. pH and Temperature Dependence of the Peroxidase-Like Activity of GNPs

The assays for pH-dependence were carried out at 25 °C in a reaction system with 50 μL of GNPs (14 nm, 47.8 $\mu g \cdot mL^{-1}$) in 200 μL of reaction buffer of different pHs (2.2, 3.0, 3.6, 4.4, 5.2, 6.0, 6.8, 7.6, 8.0, 8.3, 8.7, 9.1, 9.6, 9.8, 10.0, 10.2, 10.4, 10.6, 10.8, 11.0), in the presence of 373 mM H_2O_2 and 584 μM TMB. The reactions were monitored at 650 nm by the microplate reader every 30 s during the first 5 minutes.

Temperature assays were carried out at different temperatures (26, 32.5, 35, 37.5, 40 °C), in a reaction system with 50 μL of GNPs (14 nm, 47.8 $\mu g \cdot mL^{-1}$) and 200 μL of HAc-NaAc buffer (0.2 M, pH = 3.6) in the presence of 373 mM H_2O_2 and 584 μM TMB. The reactions were monitored at 650 nm by the microplate reader every 30 s during the first 5 minutes.

2.6. Effect of Surface Modification on Peroxidase-Like Activity of GNPs

The surface-modified GNPs were prepared by electrostatic adsorption of cationic surfactant CTAB. This was easily realized by rapidly mixing 1 mL of GNP solution (14 nm, 47.8 $\mu g \cdot mL^{-1}$) with varying amounts (1000 μL, 500 μL, 200 μL) of CTAB (5.9 $\mu g \cdot mL^{-1}$). Their UV-vis absorption spectra were measured using a 3600 spectrophotometer to monitor the surface adsorption and induced aggregation.

The catalytic experiments were carried out using the above mixture (50 μL) in 200 μL HAc-NaAc buffer (0.2 M, pH = 3.6), in the presence of 373 mM H_2O_2 and 584 μM TMB. The absorbance of the reaction solution was monitored using the microplate reader at 650 nm every 30 s during the first 5 min.

2.7. Fabrication of Gold-Antibody Nanoprobes

In this preparation, both goat anti-human IgG conjugation and BSA blocking were performed based on the electrostatic adsorption method. Before coupling with goat anti-human IgG, the pH of the GNP solution was adjusted to approximately 9.0, which is a little more than the isoelectric point of the antibody. The obtained 2 mL of GNP solution (14 nm, 47.8 $\mu g \cdot mL^{-1}$) was incubated with 100 μg goat anti-human IgG at 4 °C overnight. To remove excess antibody, conjugate solution was centrifuged at 8386 g for 40 minutes and resuspended in 2 mL of phosphate-buffered saline (PBS, pH = 7.4). After adding 100 μL 1% BSA for further blocking, the gold nanoparticle-goat anti-human IgG (GNP-GAH-IgG) nanoprobes were obtained and stored at 4 °C for use.

2.8. Procedures for the Immunoassay and Gold Staining

The immunoassay using GNP-GAH-IgG nanoprobes was performed by detecting the human IgG. 100 μL of different concentrations (0, 0.35, 1.3, 2.5, 5 $\mu g \cdot mL^{-1}$) of the analyte (human IgG, 1 $mg \cdot mL^{-1}$) diluted by carbonate/bicarbonate buffer (CB, pH 9.6) were loaded into the wells of a polystyrene 96-well microplate and incubated at 37 °C for 2 h. After washing away unbound antibody by PBS-T (pH = 7.4, Tween-20 = 0.05 volume%), the wells were blocked with 0.01 M PBS containing 1% BSA (PBS-BSA, pH 7.4). Afterwards, the wells were washed 3 times with PBS-T, and 100 μL of GNP-GAH-IgG nanoprobes were added to the wells and incubated at 37 °C for 1 h. After the wells were washed 3 times, the bottom of the wells turned light red.

100 μL of gold staining reduction solutions (2 mL of 0.01% $HAuCl_4 \cdot 4H_2O$ with 5.6 μL of 1% $NH_2OH \cdot HCl$) were added to each well and incubated at 37 °C for 14 min. Metallic gold was deposited on the GNP surfaces. The wells were washed 6 times with Milli-Q water. 100 μL of H_2O_2 (3%) was added to each well to remove the excess $NH_2OH \cdot HCl$. After the wash step was repeated 6 times, the bottom of the wells turned dark purple.

After the final wash step, 200 μL of reaction solution containing 2.07 μM TMB and 1.32 mM H_2O_2 was added to each well. The ELISA reading was performed at 650 nm by the microplate reader.

3. RESULTS AND DISCUSSION

3.1. GNPs Catalyze the Peroxidase Substrate

The colloidal solutions of 14, 25, 48, and 99 nm diameter GNPs were synthesized by the citrate reduction method. The GNPs displayed nearly spherical or ellipsoidal shape with the expected sizes (Fig. 1(a)). GNPs of different sizes have distinct UV-vis absorption spectra. The characteristic peaks of GNPs were red shifted with increasing sizes (Fig. 1(b)).

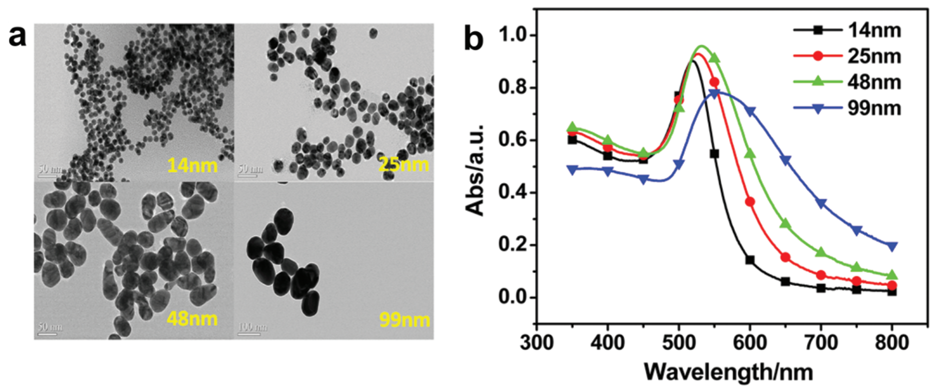

Figure 1. TEM images (a) and UV-vis spectra (b) of the gold nanoparticles with different sizes.

Using the GNPs as catalyst and TMB or ABTS as peroxidase substrates, apparent colour reactions (Fig. 2(a), blue for TMB and green for ABTS) could be generated in the presence of H_2O_2. This result indicates that GNPs display peroxidase-like activity toward typical peroxidase substrates. As the properties of inorganic nanoparticles are often dependent on size, we monitored the UV-vis absorbance-time course curves at 650 nm for TMB-H_2O_2 reaction system catalyzed by GNPs of different sizes (14, 25, 48 and 99 nm) (Fig. 2(b)). The GNPs displayed different level of activity towards TMB in the order 14 nm > 25 nm > 48 nm > 99 nm, indicating that the smaller the size, the higher the catalytic activity. The result may be due to the smaller nanoparticles having a greater surface-to-volume ratio to interact with substrates.

The peroxidase-like activity of the GNPs such as HRP, has pH and temperature dependences. We evaluated the peroxidase-like activity of the GNPs (14 nm) while varying the pH from 2 to 11 and the temperature from 26 °C to 40 °C. The optimal pH of GNPs is at a range of 3.6 to 4.8 when the substrate is TMB (Fig. 2(c)) and the relative activity reaches maximum at about 38 °C (Fig. 2(d)), which are similar to the natural enzyme of HRP. Relative activity was obtained by calculating the percentage of each absorbance data relative to the maximum absorbance measured in the experiment.

3.2. Steady-State Enzyme Kinetics

The steady-state kinetic assay of the 14 nm GNPs was monitored to investigate peroxidase-like activity.

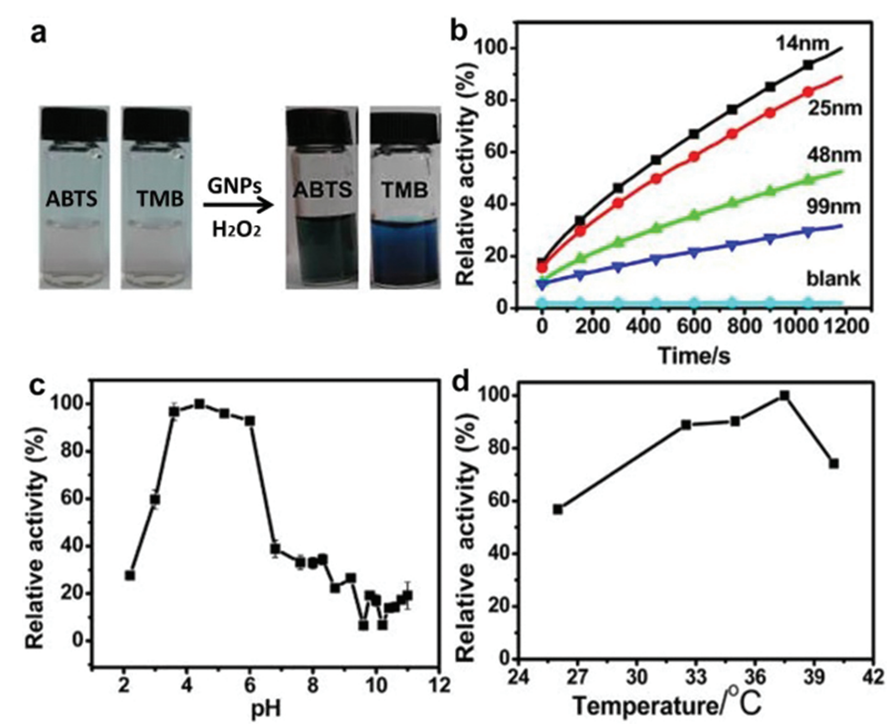

Figure 2. The different substrate (ABTS and TMB) colour reaction catalyzed by GNPs as peroxidase mimetics in the presence of H_2O_2 in HAc-NaAc buffer (0.2 M, pH = 3.6) (a). The effects of nanoparticle size (b), reaction system pH (c) and temperature (d) on the peroxidase-like activity of GNPs.

Table II. The kinetic parameters of 14 nm GNPs.

	$[E]$ (M)	Substrate	K_m (mM)	V_{max} (Ms^{-1})	K_{cat} (s^{-1})
GNPs	7.64×10^{-9}	TMB	0.20	5.59×10^{-8}	734.38
GNPs	7.64×10^{-9}	H_2O_2	572.98	9.77×10^{-8}	1,284
GNPs	3.59×10^{-10}	ABTS	92.30	3.11×10^{-8}	86.63
GNPs	3.59×10^{-10}	H_2O_2	546.60	5.04×10^{-8}	140.39

Notes: $[E]$ is the GNP concentration, K_m is the Michaelis constant, V_{max} is the maximal reaction velocity and K_{cat} is the catalytic constant, where $K_{cat} = V_{max}/[E]$. The definitions of K_m and K_{cat} are as below. The catalytic constant K_{cat} measures the number of substrate molecules turned over per enzyme molecule per second. The Michaelis constant K_m is the substrate concentration when reaction velocity reaches half of maximum reaction velocity.

The parameters obtained from the Michaelis-Menten model are shown in Table II. Lower K_m values mean tighter bonding between enzyme and substrate and more efficient catalysis. In Table II, the K_m for TMB is 0.20 mM, lower than that reported for HRP (0.434 mM),[6] which suggested that GNPs have a higher affinity for the TMB substrate than HRP. The K_m for ABTS is 92.30 mM, about 55 times higher than the K_m reported for HRP (1.67 mM).[19] The K_m value of the GNPs with TMB as the substrate is about 460 times lower than the value for ABTS, suggesting that GNPs have a higher affinity for TMB than ABTS.[20, 21] This may be due to the fact that the negatively charged citrate anions on the surface of GNPs promote electrostatic adsorption with the positively charged TMB, in contrast to the electrostatic repulsion between GNPs and ABTS. As a result, the catalytic constant K_{cat} of TMB is much higher than that for ABTS, which means each single GNP can convert more TMB into products per unit time than ABTS. In addition, we notice that the K_m value for the substrate of H_2O_2 is much larger than that reported for HRP (3.7 mM),[6] which means that a higher concentration of H_2O_2 was required to reach the V_{max} for GNPs.

3.3. The Reusability of GNPs in Catalytic Reaction

As inorganic materials, GNPs have much better thermostability and chemical stability than natural enzymes. The reusability of GNPs as peroxidase nanomimetics was investigated by detecting the characteristic peak of oxidized ABTS product at the 415 nm wavelength in the UV-vis absorption spectra for every repeated catalytic experiment. Absorbance at 415 nm wavelength showed a remarkable increase for every repeated assay (Fig. 3), suggesting an enhancement of the catalytic activity of GNPs. The insert picture showed that the absorbance of ABTS at 415 nm wavelength without catalyst was lower than that with catalyst, proving that GNPs worked on the reaction. Meanwhile, the absorption peak of GNPs was at about 521 nm, having no interference on catalyzing results. The characteristic peak of GNPs nm was red shifted and became less obvious after repeated use, which might be

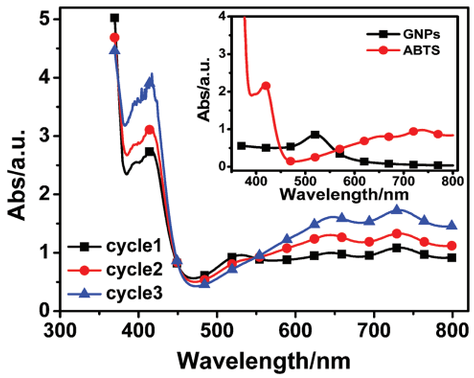

Figure 3. The UV-vis absorption spectra of catalytically oxidized products of ABTS using GNPs as peroxidase mimetics in continuous catalysis cycles in HAc-NaAc buffer (0.2 M, pH = 3.6) containing H_2O_2. GNPs showed their reusable capability, and an enhancement effect in peroxidase-like activity was observed. The inset is the controlled experiment for the UV-vis absorption spectra of GNPs and the oxidized product of ABTS without catalyst.

caused by that GNPs were activated under reaction conditions or an aggregation of GNPs appeared.[22, 23]

To investigate the mechanism of this noticeable catalytic enhancement, we firstly measured the peroxidase-like activity of the 14 nm GNPs, which had been incubated in HAc-NaAc buffer (0.2 M, pH = 3.6) to induce aggregation. HAc-NaAc buffer (0.2 M, pH = 3.6) was used because GNPs are sensitive to high concentrations of electrolytes (Fig. 4(a)). Unfortunately, the longer the GNPs were incubated, the higher their aggregation level and the lower their peroxidase-like activity. Then, as shown in Figure 4(b), H_2O_2 treatment was demonstrated to be able to enhance the peroxidase-like activity of GNPs, which is probably responsible for the activity increase in a circular catalytic reaction by reduplicative use of GNPs. Natural enzymes must be immobilized to be reused, and this might decrease their activity after repeated assays.[24] The colour of GNPs turned purple until the fifth centrifugal process and the catalytic activity decreased subsequently because of excessive H_2O_2 treatment and serious aggregation. Our study indicates that, the reusable and activity-increasing speciality of GNPs is more advanced than natural enzymes.

3.4. Effect of Surface Modification on the Peroxidase-Like Activity of GNPs

The peroxidase-like activities of GNPs with and without CTAB modification were measured (Fig. 5(a)). As reported, the CTAB micelles themselves have intrinsic catalytic activity[25, 26] that is less than the intrinsic catalytic activity of GNPs (Fig. 5(a)). However, the peroxidase-like activity of GNPs abated after CTAB surface modification compared to GNPs and CTAB alone. To investigate this, we modified GNPs with different amounts of CTAB. The absorption peaks of GNPs coated with 1,000 μL of CTAB solution (5.9 $\mu g \cdot mL^{-1}$) had an extremely tiny red shift,

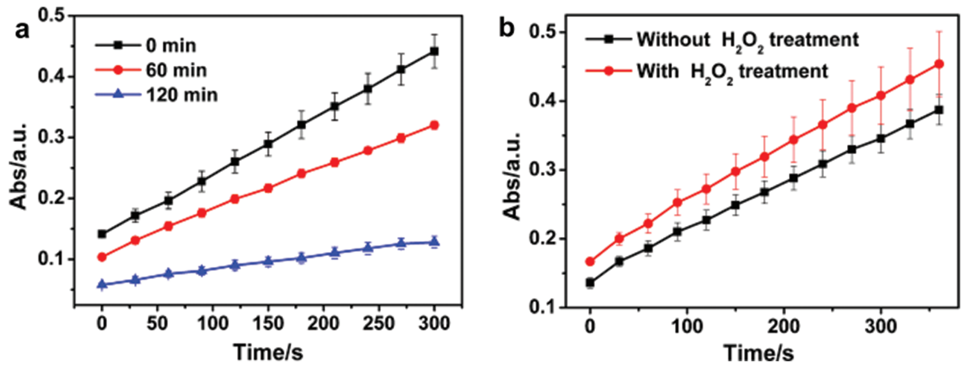

Figure 4. (a) The effect of particle aggregation on the peroxidase-like activity of GNPs. In order to induce particle aggregation, GNPs were incubated for different times (0 min, 60 min and 120 min, respectively) in an HAc-NaAc buffer (0.2 M, pH = 3.6), to which substrates of ABTS and H_2O_2 were then added. Absorbance-time course curves were recorded. (b) The effect of GNP pretreatment with H_2O_2 on the peroxidase-like activity of GNPs. GNPs were incubated in HAc-NaAc buffer (0.2 M, pH = 3.6) containing 9.79 M H_2O_2 for 10 min, then were dialyzed in ultrapure water to remove remaining H_2O_2. The peroxidase-like activity was evaluated using ABTS and H_2O_2 as substrates in HAc-NaAc buffer for GNPs without any treatment and with H_2O_2 treatment, respectively.

compared to the peaks of GNPs without CTAB modification in UV-vis absorption spectra (Fig. 5(b)). There probably was a CTAB bilayer formed on the GNP surface (see inset in Fig. 5(b)) when the GNPs were blended rapidly with excessive CTAB. The surface of this structure was hydrophilic and prevented aggregation, so there was almost no change for the characteristic peak. The peaks of the other two samples were obtained at 550 nm and 600 nm when GNPs were mixed with 500 μL and 200 μL of CTAB (5.9 $\mu g \cdot mL^{-1}$), respectively. The probable reason was that a hydrophobic monolayer was formed on GNPs because of lack of CTAB, then GNP aggregation was induced and the characteristic GNP peak was red shifted. The CTAB bilayer that blocked catalytic activity sites on the GNPs prevented interaction between the GNPs and TMB, so the catalytic activity of the GNPs decreased after they were modified (Fig. 5(a)).

3.5. Application of the Immunoassay and Gold Staining Enhancement

We used GNPs instead of HRP for ELISA assays and developed the gold staining method to enhance the detection sensitivity of ELISA (Fig. 6). We constructed the GNP-GAH-IgG nanoprobes by coating GNPs with goat anti-human IgG, which acted as both a specific label and a peroxidase mimetic that catalyzed the colour reaction of substrate TMB. As for conventional gold-labeled ELISA without using gold staining, the human IgG was placed in a 96-well plate and GNP-GAH-IgG nanoprobes were added to label the human IgG. The nonspecific bonding was removed with several washes, then the substrate solution containing TMB and H_2O_2 was added to generate a colour reaction.

The appropriate concentration of H_2O_2 used in the ELISA application was first examined, as shown in Figure 7(a), which indicates that GNP-GAH-IgG nanoprobes require a high H_2O_2 concentration to reach maximal peroxidase activity. However, the excessive H_2O_2 concentration could lead to a direct colour reaction with TMB in the absence of the GNP-GAH-IgG nanoprobes, which easily caused false positive results. Since the capacity of the microplate well is 300 μL, we added 200 μL of the substrate solution per well, leading to a final H_2O_2 concentration of 1.3 mM, when human IgG was detected using GNP-GAH-IgG nanoprobes with relatively high sensitivity. Their absorbance at 650 nm was recorded as a

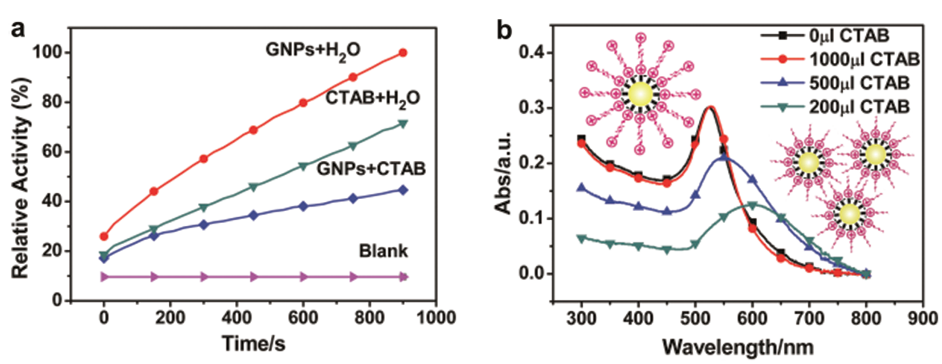

Figure 5. (a) The effect of surface modification with CTAB on the peroxidase-like activity of GNPs. (b) The effect of surface modification with CTAB on the UV-vis absorption spectra of GNPs.

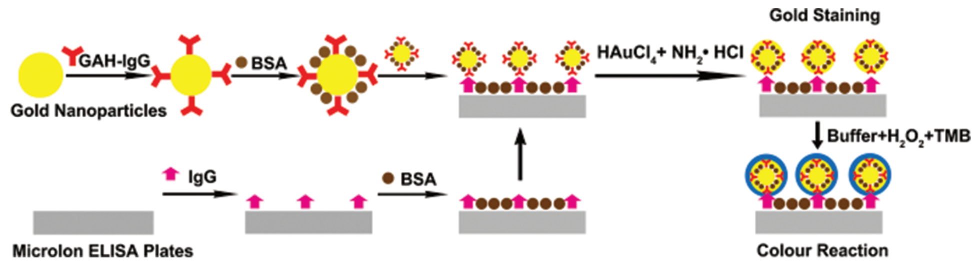

Figure 6. Schematic illustration of gold nanoprobe preparation and the gold-staining-enhanced ELISA process.

function of IgG concentration (0 ng · well^{-1} as blank group, 30–500 ng · well^{-1} as experimental groups) (Fig. 7(b)).

As mentioned in above study, the catalytic activity of GNPs was weakened by surface modification with CTAB. The peroxidase-like activity of GNPs coated with goat anti-human IgG (or goat anti-human IgG and BSA) was measured (Fig. 8). The activity of GNPs coated with goat anti-human IgG was lower than those without coating and GNPs coated with both goat anti-human IgG and BSA was the lowest. Therefore, the phenomenon would result in a lower detection sensitivity for the established ELISA method. A more sensitive enzyme immunoassay method using gold nanoprobes combined with gold staining (Fig. 6) was investigated. The method was based on the catalytic reduction of Au^{3+} by hydroxylamine hydrochloride ($NH_2OH \cdot HCl$) and the subsequent deposition of gold atoms on the gold nanoprobes, which produced a freshly exposed gold catalytic surface with relatively high peroxidase-like activity as demonstrated below.

To determine optimum gold staining time, we performed gold staining experiments of different times. The positive group (250 ng · well^{-1} human IgG + BSA blocking) and negative group (0 ng · well^{-1} human IgG + BSA blocking) were set to obtain the positive/negative (P/N) ratio. Because the Au^{3+}-$NH_2OH \cdot HCl$ reduction solutions were not stable at room temperature, they began to turn from colourless to red 16 min later so we selected a maximum staining time of 14 min, which avoided the colour change of the solution itself and produced the maximum P/N ratio as well, as shown in Figure 9(a). Using 14 min as an optimal gold staining time, we achieved more sensitive detection results for human IgG in a lower concentration range of 0–70 ng · well^{-1} (Fig. 9(b)). After the gold staining, the absorbance is about 7 times higher than that obtained in Figure 7(b), when the human IgG concentration is 70 ng · well^{-1}. These experiments demonstrate that GNPs are both catalysts and intensive probe tools. Their novel peroxidase-like activity and the gold staining method allow GNPs to detect other biomolecules, especially low levels of biomolecules using the established ELISA method.

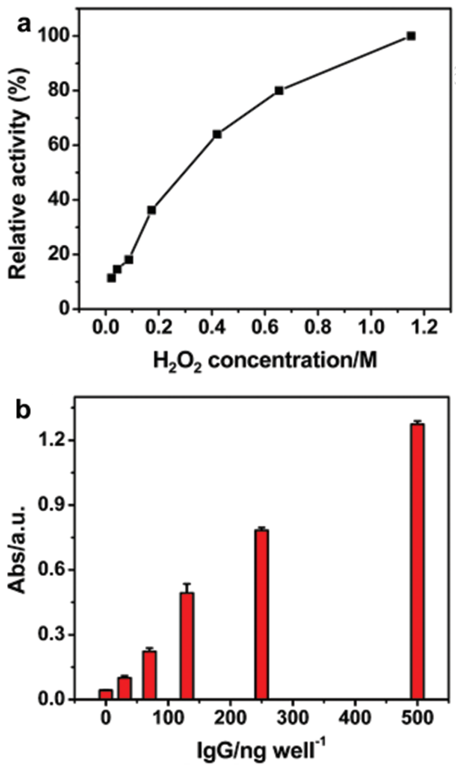

Figure 7. (a) The H_2O_2 concentration dependence of the peroxidase-like activity of GNPs. A high H_2O_2 concentration was required to reach high detection sensitivity for ELISA application. The maximum point was set as 100%. (b) With 1.3 mM H_2O_2, the UV-vis absorbance (650 nm) depends on the concentration of human IgG over the range of 0–500 ng · mL^{-1}. (Conditions: 0.2 mM pH 3.6 NaAc buffer + 0.5 μM TMB + 1.3 mM H_2O_2).

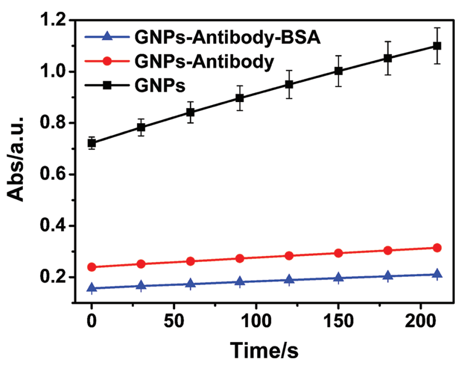

Figure 8. The influence of antibody conjugation and BSA blocking on the absorbance time course for the GNP-catalyzed colour reaction using ABTS and H_2O_2 as substrates in 0.2 M HAc-NaAc buffer (0.2 M, pH = 3.6). The peroxidase-like activity of GNPs that were modified with goat anti-human IgG and BSA is markedly lower than that of GNPs that were not modified.

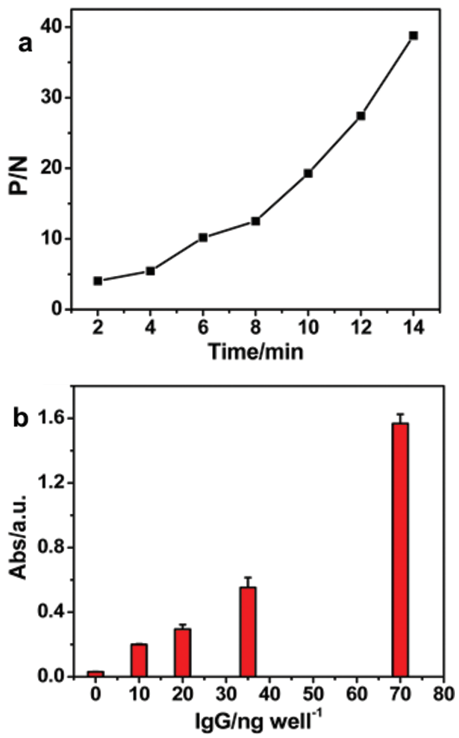

Figure 9. (a) The positivity/negativity ratio (P/N) increases with gold staining time when GNP-GAH-IgG nanoprobes are used to detect human IgG, suggesting that gold staining can enhance detection sensitivity. (b) By gold staining for 14 min, the relationship between absorbance at 650 nm and human IgG concentration (0–70 ng · well^{-1}) was obtained with much higher sensitivity than the results in Figure 7.

4. CONCLUSIONS

We evaluated the peroxidase-like activity of GNPs. The peroxidase-like catalysis of GNPs followed Michaelis-Menten kinetics and was dependent on the environmental pH, temperature, and the size and surface modifications of the GNPs. The peroxidase-like activity of GNPs could be enhanced by H_2O_2 treatment, resulting thus in the activity increase in a circular catalytic reaction. We also designed and evaluated GNPs for ELISA applications. When used in an immunoassay, the surface of GNPs are usually covered with antibodies and other biomacromolecules, which blocks the catalytic active sites and reduces the catalysis ability of GNPs dramatically. To get fresh, exposed gold catalyst surface, we developed a gold staining method that increases the assay's sensitivity and avoids the negative effects of surface modifications. The colorimetric analysis is simple, cheap and rapid, which provides significant improvement for the immunoassay.

Acknowledgment: We would like to thank Barbara Berman for editorial assistance. This research was supported by the National Basic Research Program of China (No. 2011CB933503), the National Natural Science Foundation of China (No. 31170959, 81071419), the Research Program of Jiangsu Province (Nos. BK2011036, SBC201310643 and BL2013029), the Research Fund for the Doctoral Program of Higher Education of China (20110092110029), and was partially supported by a regulatory science grant under the FDA Nanotechnology CORES Program and by the Office of Cosmetics and Colors, CFSAN/FDA (Junjie Yin). This article is not an official U.S. Food and Drug Administration (FDA) guidance or policy statement. No official support or endorsement by the U.S. FDA is intended or should be inferred.

References and Notes

1. R. K. Singh, M. K. Tiwari, R. Singh, and J. K. Lee, *Int. J. Mol. Sci*. 14, 1232 (**2013**).
2. R. Beynon and J. Kay, *Biochem. J*. 173, 291 (**1978**).
3. Z. F. Zhang, H. Cui, C. Z. Lai, and L. J. Liu, *Anal. Chem*. 77, 3324 (**2005**).
4. F. E. Kruis, H. Fissan, and A. Peled, *J. Aerosol. Sci*. 29, 511 (**1998**).
5. Z. Q. Li, W. Y. Li, P. H. C. Camargo, and Y. N. Xia, *Angew. Chem. Int. Ed*. 47, 9653 (**2008**).
6. L. Z. Gao, J. Zhuang, L. Nie, J. B. Zhang, Y. Zhang, N. Gu, T. H. Wang, J. Feng, D. L. Yang, S. Perrett, and X. Y. Yan, *Nat. Nanotechnol*. 2, 577 (**2007**).
7. R. André, F. Natálio, M. Humanes, J. Leppin, K. Heinze, R. Wever, H. C. Schröder, W. E. G. Müller, and W. Tremel, *Adv. Funct. Mater*. 21, 501 (**2011**).
8. X. Q. Zhang, S. W. Y. Gong, Y. Zhang, T. Yang, C. Y. Wang, and N. Gu, *J. Mater. Chem*. 20, 5110 (**2010**).
9. Y. J. Guo, L. Deng, J. Li, S. J. Guo, E. K. Wang, and S. J. Dong, *ACS Nano* 5, 1282 (**2011**).
10. J. Fan, J. J. Yin, B. Ning, X. C. Wu, Y. Hu, M. Ferrari, G. J. Anderson, J. Y. Wei, Y. L. Zhao, and G. J. Nie, *Biomaterials* 32, 1611 (**2010**).
11. W. W. He, Y. Liu, J. S. Yuan, J. J. Yin, X. C. Wu, X. N. Hu, K. Zhang, J. B. Liu, C. Y. Chen, Y. L. Ji, and Y. T. Guo, *Biomaterials* 32, 1139 (**2011**).
12. A. Ravalli and G. Marrazza, *J. Nanosci. Nanotechnol.* 15, 5524 (**2015**).
13. C. C. Lin, Y. C. Yeh, C. Y. Yang, C. L. Chen, G. F. Chen, C. C. Chen, and Y. C. Wu, *J. Am. Chem. Soc*. 124, 3508 (**2002**).
14. R. J. Cui, H. P. Huang, Z. Z. Yin, D. Gao, and J. J. Zhu, *Biosensors and Bioelectronics* 23, 1666 (**2008**).
15. Z. D. Wang, J. H. Lee, and Y. Lu, *Adv. Mater*. 20, 3263 (**2008**).
16. S. Alex and A. Tiwari, *J. Nanosci. Nanotechnol.* 15, 1869 (**2015**).
17. W. W. He, Y. T. Zhou, W. G. Wamer, and J. J. Yin, *Biomaterials* 34, 765 (**2013**).
18. G. Frens, *Nature Physical Science* 241, 20 (**1973**).
19. P. Vanachayangkul and W. H. Tolleson, *Enzyme Research* 2012, 1 (**2012**).
20. F. Yu, Y. Huang, A. J. Cole, and V. C. Yang, *Biomaterials* 30, 4716 (**2009**).
21. S. Wang, W. Chen, A. Liu, L. Hong, H. Deng, and X. Lin, *ChemPhysChem*. 13, 1119 (**2012**).
22. U. Kreibig and L. Genzel, *Surf. Sci*. 156, 678 (**1985**).
23. D. Aili, K. Enander, J. Rydberg, I. Lundstrom, L. Baltzer, and B. Liedberg, *J. Am. Chem. Soc*. 128, 2194 (**2006**).
24. E. T. Farinas, T. Bulter, and F. H. Arnold, *Curr. Opin. Biotechnol*. 12, 545 (**2001**).
25. L. S. Romsted, C. A. Bunton, and J. H. Yao, *Curr. Opin. Colloid. In*. 2, 622 (**1997**).
26. T. J. Broxton, J. R. Christie, and R. Chung, *J. Org. Chem*. 53, 3081 (**1988**).

Received: 13 June 2016. Accepted: 27 October 2016.